

Article

Not peer-reviewed version

A Conclusive Model-Fit Current-Voltage Characteristics Curves with Kink Effects

[Hsin-Chia Yang](#)^{*} and Sung-Ching Chi

Posted Date: 13 July 2023

doi: 10.20944/preprints202307.0933.v1

Keywords: Keywords: kink effect, solitary wave, phonons



Preprints.org is a free multidiscipline platform providing preprint service that is dedicated to making early versions of research outputs permanently available and citable. Preprints posted at Preprints.org appear in Web of Science, Crossref, Google Scholar, Scilit, Europe PMC.

Copyright: This is an open access article distributed under the Creative Commons Attribution License which permits unrestricted use, distribution, and reproduction in any medium, provided the original work is properly cited.

Article

A Conclusive Model-Fit Current-Voltage Characteristics Curves with Kink Effects

Hsin-Chia Yang *, Sung-Ching Chi

Department of Electronic Engineering, Ming Hsin University of Science and Technology, Hsinchu 30401, Taiwan; chisc@must.edu.tw

* Correspondence: hcyang@must.edu.tw

Abstract: Current-voltage characteristics curves of NFinFET are presented and are fitted with the modified current-voltage (I-V) formulas, where the modified term in the triode region is demonstrated to be indispensable. In the as-known I-V formula, important parameters need determining to make both the measured data and the fitting data as close as possible. Those parameters include k_N (associated with the sizes of the transistor and mobility), λ (associated with Early Voltage), and V_{th} (the threshold voltage). The differences between the measured data and the fitting data vary as the applied source-drain bias, proving that the mobility of the carriers not consistently constant. On the other hand, a modified formula, called kink effect factor, is negatively or positively added simulating solitary heat waves or lattice vibration, which disturb the propagation of carriers and thus influence the Source-Drain current (I_{DS}). The new statistical standard deviations (δ) are then found to be effectively suppressed as the kink effect is taken into account.

Keywords: kink effect; solitary wave; phonons

1. Introduction

Transistors fabricated in semiconductor industry successfully achieve various desired functions, including signal processing, data calculating, and decision-making. All the functions are associated with memory transferring at a comparable speed. So the size of transistor continues to shrink not mainly for the benefits of increasing number of integrated circuit (IC). The speed of IC's somehow becomes the pursuing goal. Three concerns appear manifested in a sense. They are outrageous loss of controllability, unavoidable heat, and un-expected limitation of photolithograph. The controllability is closely related to leakage current due to proportional dimension shrinkage even though some adopted prevention including halo implant or pocket implant has been done at the planar device level. In addition, the promotion of electrical performance at the same scale using compressive or tensile stress technique is seriously taken into account as well. Unfortunately, channel lengths below tens of nanometers seem not to work out any more as desired no matter what has been taken. Instead of planar bulk silicon substrate, there comes the 3-D structural fin-like field effect transistor (FinFET), which make use of slim strip of epitaxial silicon as body substrate wrapped by insulator-separated gate poly-silicon. The strip of channel substrate gets depleted as the gate poly-silicon is applied with a bias. This bias causes the depletion region of the substrate strip impressively and effectively to block the leakage current in between Source and Drain. As for the generated heat, it is basically linked to the equivalent resistors, whose resistance is actually proportional to the length of the resistor and inversely dependent of the area of the cross section. The resistance of decreasing dimension soars up making the increasing Ohm's heat tremendously degrade its electrical performance and thus competitively loss leading status. Therefore, the conduction of heat dominates the whole process flow and material choosing. Copper is thus preferred for its higher conductivity. The expose of ultra-violet ray suggests diffraction immunity, which is identified as the use of shorter wavelength, improvement of refraction angle (refractive index, n), and subtle design and combination of masks. Traditional optics and modern optics are both utilized or designed to resolve diffraction issues.

Furthermore, the electrical performances for any transistor have to be reliable and repeatable. Models are thus proposed to address the electrical performances and are able to fit the measured characteristics curves. And all the circuit designs, including analog and digital, rely solely on the established model. Research has to be paid to understand the electrical data. The most commonly used formulas have been posed for over many decades, and they surely reduce the tremendous work on the designing level. Therefore, the current-versus-voltage characteristic curves showing electrical performance of transistors are necessarily parameter-extracted in the model. Nevertheless, ones are still intrigued to know if the “modified” conventional formula is applicable for fitting repeated characteristic curves. [1–14] In the model, useful parameters are supposed to be constants even though they need interpreting. Some evidences in this paper do show some limitation. For example, the mobility is no longer reasonably treated as constant as the measured data are compared to the modified conventional formula.

Furthermore, one thing that causes attention is about carriers traveling in the crystallized silicon, which is diamond structure. The crystal thermally vibrates at certain temperature causing trouble to the carriers. As the carriers speed up, they confront more obstacles. More obstacles generate more heat and more friction, which may slow down the carriers, especially in the triode region. For example in our daily life, the rain falls at the almost constant terminal speed near the ground addressing the similar situation. The lattice interacts with the carriers and is energetically quantized as phonons, which is analogous to photons in electrical magnetic field. The analogy becomes good referencing facts that are readily explored.

In this study, the as-measured (I_{DS} , V_{DS}) data are referred to the transistors fabricated by 3-D FinFET structure process. The “modified” conventional I-V characteristic curve formulas in Equation (1) with λ (the inverse of the absolute value of Early voltage, V_A) is deliberately introduced in the triode region for V_{DS} is less than $(V_{GS} - V_{th})$, whereas Equation (2) is kept unchanged for the saturation regime. Delta deviation in Equation (3) for the whole fitting is suggested and effectively reduced the discrepancy between the fitting data and the measured data. In addition, a solution to a non-linear differential equation, called the sine-Gordon equation, is first proposed for addressing a solitary wave, which is some kind of phonons coming from quantized sound. The solution is proven to be Gaussian and is introduced to further reduce the delta deviation in the electrical characteristic curves, which is really encouraging.

2. Preparation of as Measured Data and Fitting

2.1. Preparation

The as measured (I_{DS} , V_{DS}) data is obtained through the probe station on the FinFET technology, which uses epitaxial silicon grown on silicon wafer and an dry-etched floated island “I” with two head ends as Source and Drain and the channel in between two ends. Dry oxidation of 14 angstroms on the slim sides followed by 4000 angstrom poly-silicon as Gate functions the transistor looking like a fin after dry-etching. The measured data and the self-generated data coming from the modified conventional formulas in Equations (1) and (2) as followed in the next paragraph are merged into one graph for comparison of fitting.

2.2. Fitting I_{DS} - V_{DS} and I_{DS} - V_{GS}

For MOSFET devices, the commonly conventional formulas are modified as follows:

$$I_{DS}(Triode) = k_N[(V_{GS} - V_{th})V_{DS} - \frac{V_{DS}^2}{2}](1 + \lambda V_{DS}) - \alpha \exp[-\beta(V_{DS} - \chi)^2] \quad (1)$$

and

$$I_{DS}(\text{Saturation}) = k_N \frac{(V_{GS} - V_{th})^2}{2} (1 + \lambda V_{DS}) - \alpha \exp[-\beta(V_{DS} - \chi)^2] \quad (2)$$

where

$$k_N = \frac{C_{ox} W \mu}{L_o}$$

and

$$\lambda = \frac{1}{|V_A|}$$

C_{ox} is the gate capacitance, W and L_o are the width and the length of the transistor, and μ is the mobility of carriers. Also V_A means Early Voltage, α is the kink effective coefficient, and β and χ are the corresponding speed-associated values.

For one thing, it is worth mentioning that the term $(1 + \lambda V_{DS})$ in Equation (1) is necessarily added because, with or without it, the differences on fitting are demonstrated as in Figure 1.

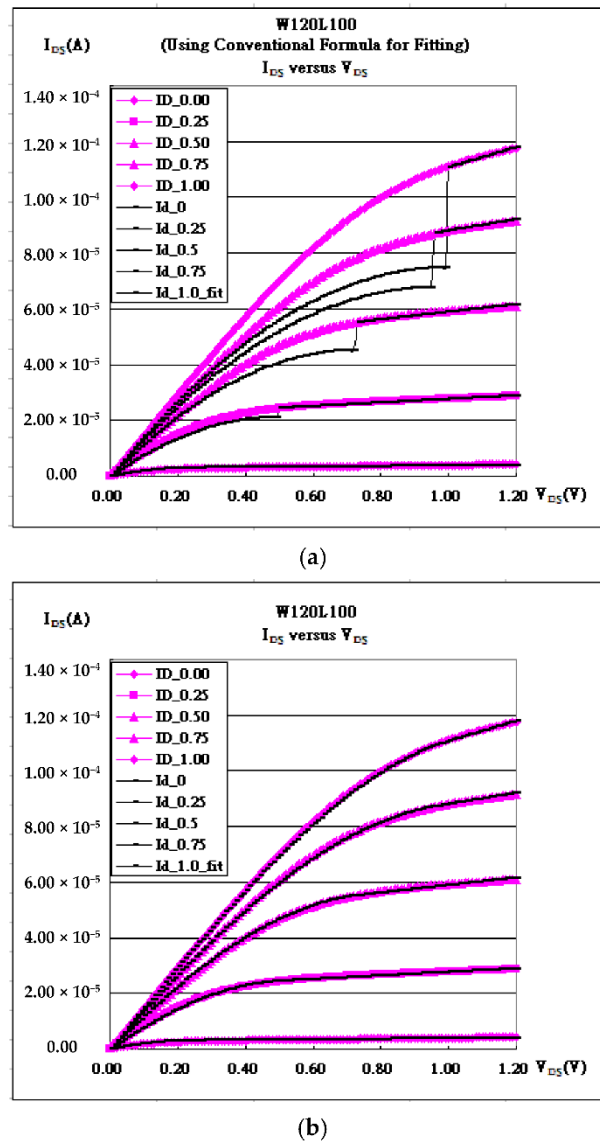


Figure 1. I_{DS} - V_{DS} characteristic curves and the corresponding fitting (a) without taking the term $(1 + \lambda V_{DS})$ in Eq.(1) into account. (b) with taking the term $(1 + \lambda V_{DS})$ in Equation (1) into account.

2.3. The Delta Deviation

The fitting data by Equations (1) and (2) are deliberately used to fit the as-measured I-V characteristic curves. Those parameters are mainly determined predominantly according to the minimum delta (δ) in the following Equation (3):

$$\delta = \sqrt{\frac{\sum_{i=1}^N (I_{\text{fitting}} - I_{\text{measured}})_i^2}{N}} \quad (3)$$

For example, the final value of k_N is determined to be $1.49 \times 10^{-4} (1/V^2)$ through the smiling curve as the minimum delta is located in Figure 2. [15,16]

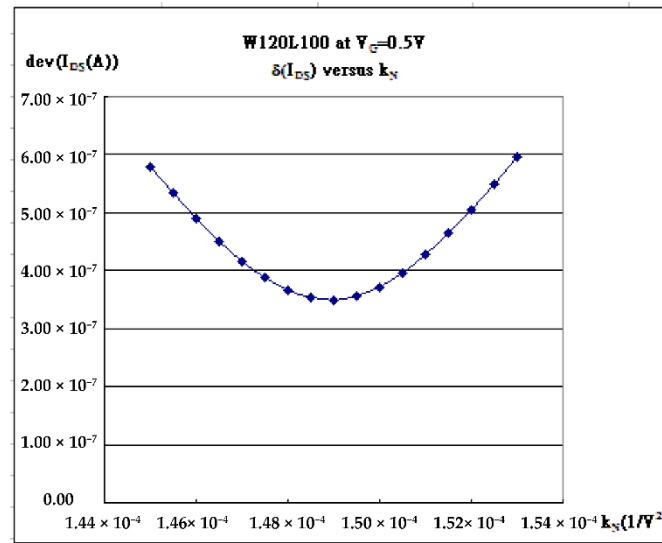


Figure 2. I_{DS} - V_{DS} characteristic curves and the corresponding fitting with minimum delta (δ) skill in the following Equation (3)

2.4. The kink effect

The non-linear differential equation addressing a moving electron scalar field in the strongly inversed layer is presented as follows:

$$\frac{\partial^2 \phi_e}{c^2 \partial t^2} - \frac{\partial^2 \phi_e}{\partial x^2} + a \sin b \phi_e = 0 \quad (4)$$

which is named as sine-Gordon equation. [17] The moving electrons accelerated by the electrical field confront phonons with group velocity c of thousands of meters per second in the lattice [18]. The space-time variables are adjusted with respect to the referencing frame as follows:

$$\phi_e(x, t) = f_e(x - vt) = f_e(\xi)$$

Equation (4) thus reduces to the following form:

$$\frac{\partial^2 \phi_e}{\partial \xi^2} - a(1 - \frac{v^2}{c^2})^{-1} \sin b \phi_e = 0 \quad (5)$$

The non-linear solution of Equation (5) is expressed as

$$f_e(\xi) = \frac{4}{b} \arctan e^{\pm \gamma \xi} \quad (6)$$

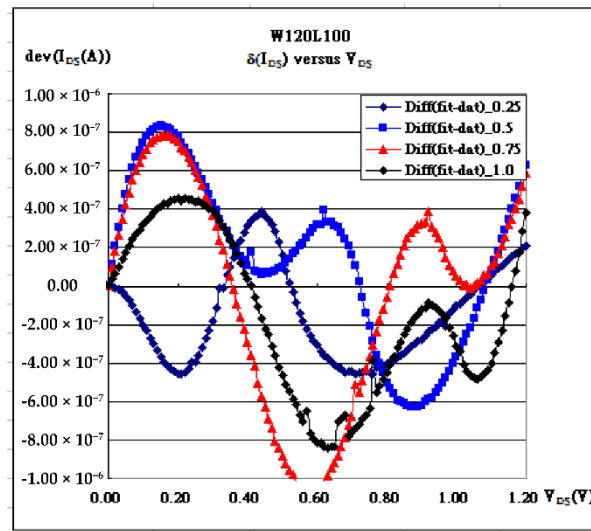
where

$$\gamma = (1 - \frac{v^2}{c^2})^{-1/2}$$

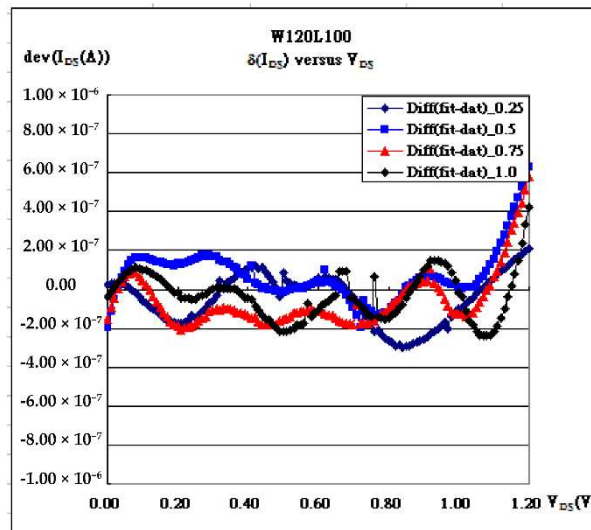
The speed of the electron, closely associated with current density ($J=nev$), is proportional to the derivative of the wave function with respect to ξ .

$$\begin{aligned} \frac{df(\xi)}{d\xi} &= \frac{(4/b)\gamma e^{\gamma\xi}}{1+e^{2\gamma\xi}} = \frac{(4/b)\gamma}{e^{\gamma\xi} + e^{-\gamma\xi}} \\ &\rightarrow (2/b)\gamma(1 - \frac{\gamma^2\xi^2}{2}) \rightarrow (2/b)\gamma \exp[-\frac{\gamma^2\xi^2}{2}] \end{aligned} \quad (7)$$

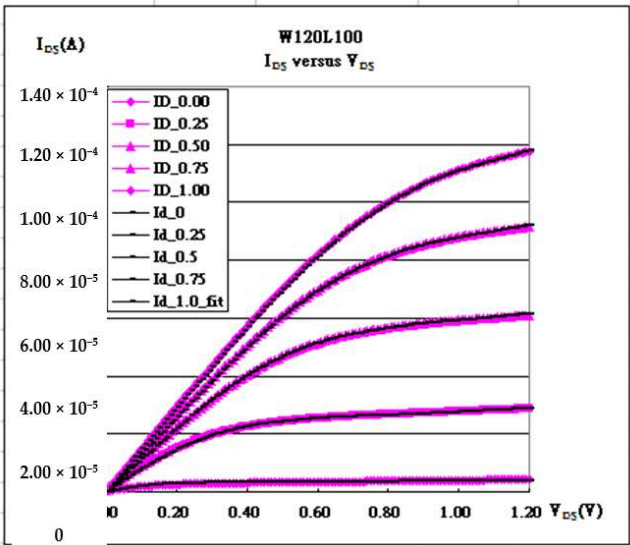
Therefore, the fine variations of I_{DS} in Figure 3a are to be easier modified by using the above Gaussian form, followed by Figure 3b with less minimum delta. The final fitting curves are then as shown in Figure 3c.



(a) $\delta_{0.25}=2.86 \times 10^{-7}$, $\delta_{0.5}=4.50 \times 10^{-7}$, $\delta_{0.75}=5.64 \times 10^{-7}$, $\delta_{1.0}=4.38 \times 10^{-7}$ referring to Figure 1b



(b) advanced: $\delta_{0.25}=1.37 \times 10^{-7}$, $\delta_{0.5}=1.55 \times 10^{-7}$, $\delta_{0.75}=1.57 \times 10^{-7}$, $\delta_{1.0}=1.25 \times 10^{-7}$



(c) advanced

Figure 3. (a) The subtraction values of I_{DS} - V_{DS} characteristic curves and the corresponding fitting without taking the Gaussian term into account. (b) with taking the Gaussian term into account. (c) the corresponding fitting in Figure 3b

3. Application

The minimum delta (δ) in Equation (3) can be used to determine the chosen parameters with or without taking kink effects into account, which are listed in Tables 1 and 2. [8] In both tables, the minimum delta at different Gate biases requires different k_n , lambda (λ), and threshold voltages. For one thing, both Table 1 and Table 2 have reasonable delta trends; the higher the V_{GS} is, the higher the delta is because of larger scales. Furthermore, the fitting with kink effects is apparently superior to the one without. As referred to Figure 4, the fitting is not as good. Once the curves are enlarged in Figure 4b, the fitting curves do not consistently match the as measured data. Therefore, the minimum delta shown in Table 1 is usually at the order of 10^{-6} , except $V_G=1.0$ Volt.

With taking kink effects into account as shown in Table 2, the deviation (delta) can be suppressed as lowly as 10^{-7} , and the fitting is improved a lot in Figure 5. When turning off kink effects as shown in Figure 5a,b, the fitting curves are always lifted up at $V_{DS} \sim (V_{GS} - V_{th})$ as compared to the as measured data. To take care of the issue on which fitting curves are commonly lower than as-measured currents, the kink effects are thus considered. The solitary waves can be in thermal form, or maybe in phonons. The electron might be deflected because of the collisions with phonons, and those collisions may cause degradation of electrical performances. The item is thus introduced and subtracted, which is proportional to the exponential with the Gaussian form, as seen in Equation (1) and Equation (2). In Figure 5c,d, the fitting is really encouraging. The enlarged figure in Figure 5d does enhance the fitting.

Table 1. Transistors Using 0.25 micron Process Technology without Kink Effect Factor

Gate Bias	k_n	V_{th_fit}		
$V_G=1.00V$	2.080×10^{-4}	0.5275	0.138	5.9311×10^{-7}
$V_G=2.00V$	3.181×10^{-4}	1.1437	0.073	1.6219×10^{-6}
$V_G=3.00V$	3.547×10^{-4}	1.9238	0.075	2.3925×10^{-6}
$V_G=4.00V$	2.859×10^{-4}	2.5900	0.079	2.3448×10^{-6}
$V_G=5.00V$	2.151×10^{-4}	3.2157	0.099	3.3145×10^{-6}

Table 2. Transistors Using 0.25 micron Process Technology with Kink Effect Factor

Gate Bias	k_N	V_{th_fit}		
$V_G=1.00V$	2.260×10^{-4}	0.5275	0.082	2.2803×10^{-7}
$V_G=2.00V$	3.365×10^{-4}	1.1437	0.040	6.5269×10^{-7}
$V_G=3.00V$	3.850×10^{-4}	1.9238	0.030	6.8806×10^{-7}
$V_G=4.00V$	3.060×10^{-4}	2.5900	0.044	7.6246×10^{-7}
$V_G=5.00V$	2.296×10^{-4}	3.2157	0.065	8.9941×10^{-7}

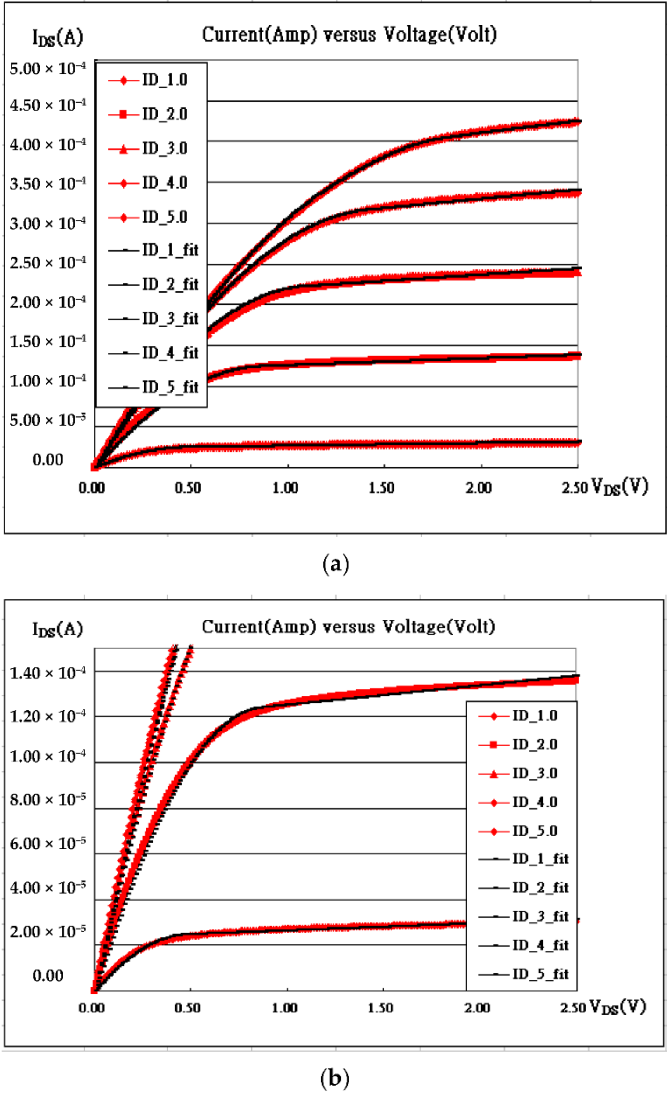
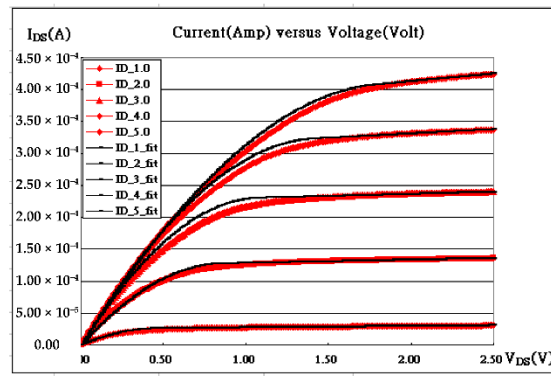
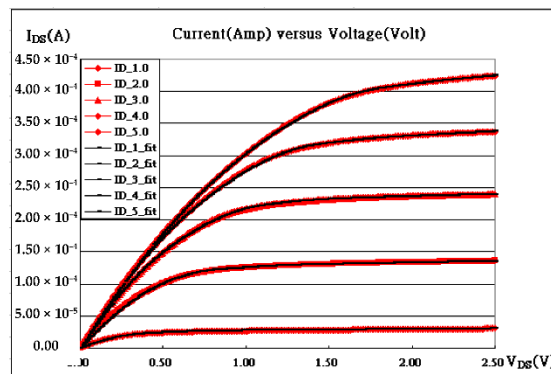


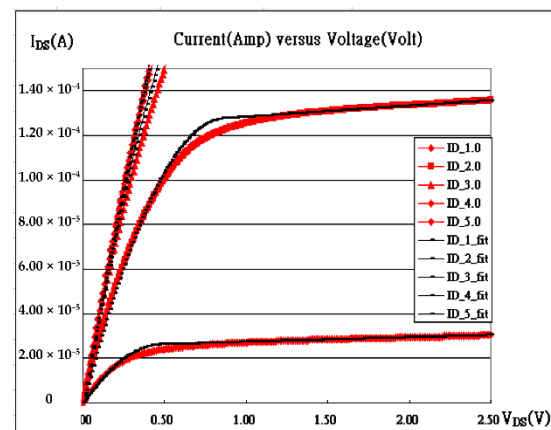
Figure 4. 0.25 micron process (a) I_{DS} - V_{DS} characteristic curves and the corresponding fitting without taking kink-effect factor into account. (b) Enlarged I_{DS} - V_{DS} characteristic curves and the corresponding fitting without taking kink-effect factor into account.



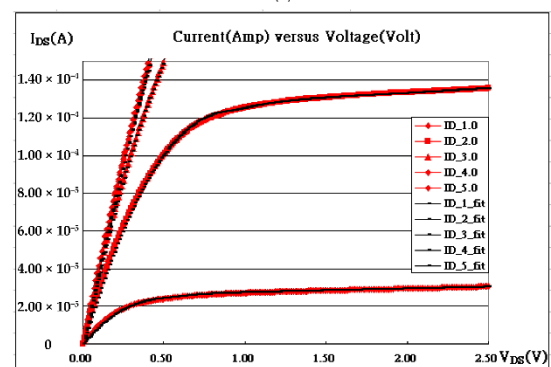
(a)



(b)



(c)



(d)

Figure 5. 0.25 micron process (a) I_{DS} - V_{DS} characteristic curves and the corresponding fitting by turning off kink-effect factor. (b) I_{DS} - V_{DS} characteristic curves and the corresponding fitting by turning on kink-effect factor. (c) Enlarged I_{DS} - V_{DS} characteristic curves and the corresponding fitting by turning off kink-effect factor. (d) Enlarged I_{DS} - V_{DS} characteristic curves and the corresponding fitting by turning on kink-effect factor.

4. Conclusions

The as measured data redrawn as characteristic curves can be fitted with the ones based on the modified conventional current-voltage formula. Even though it is quite engineering, such a fitting may be quite easy to be undertaken because all the parameters do not have to be the same and are easily adjusted. Instead, the trends or scales of some specific parameter always give some thoughts. On the other hand, the kink effect does really exist as referred to Figure 5a,c for 0.5 micron process and, furthermore, Figure 6a,b for 0.09 micron process, and it shall efficiently help to work out the fitting as referred to Figure 5b,d, and Figure 7a,b, where the minimum delta (δ) is proven to effectively reduce as expected.

Fitting with Kink effects gives the idea that the mobility implicitly shown in k_N varies all the time correlating to the subtractions in Figure 3a,b while the gate capacitance and the effective channel length and width shall be reasonably treated as fixed quantities. In the conventional model, the mobility included in k_N is supposed to be averagely constant, which is, in turn, unable to be convincing. Therefore, the mobility is then proven to be a variant along the strongly-inversed channel length. In addition, all the kink modified terms in Equation (7) for the fitting demonstrate that the values of $(-\gamma^2/2)$ are about tens, e.g., (-50) . That is to say, the velocity of electron is quite the same order of the group velocity of the phonon, thousands of meters per second.[18]

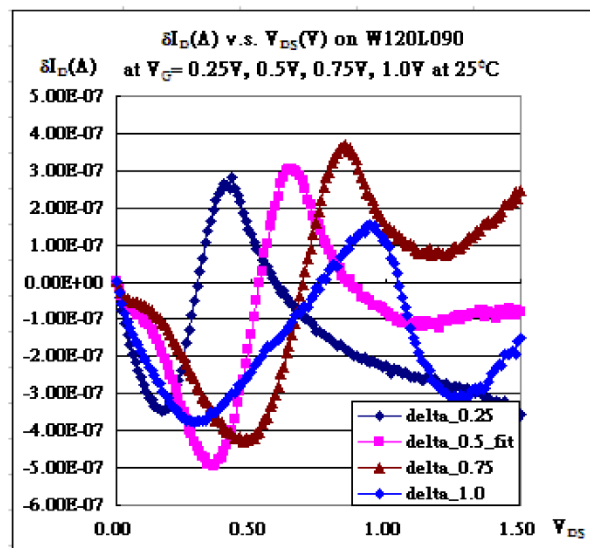
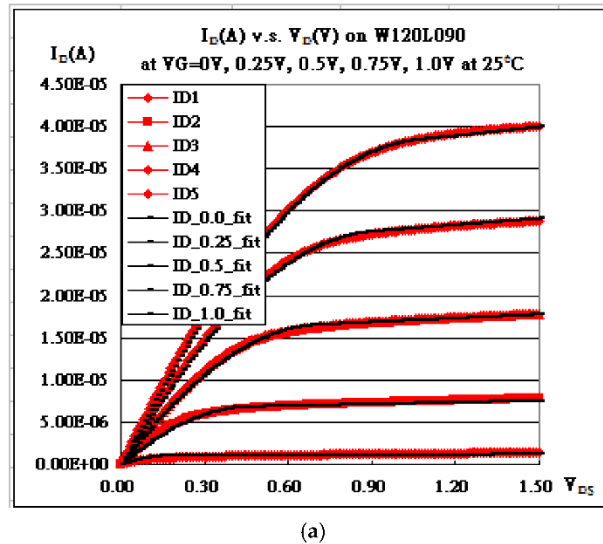
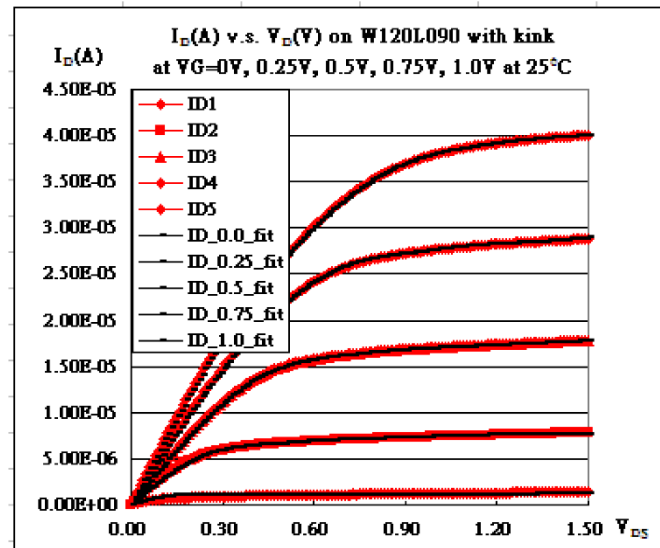


Figure 6. 0.090 micron process (a) I_{DS} - V_{DS} characteristic curves and the corresponding fitting without taking kink-effect factor into account. (b) the corresponding fitting with minimum delta (δ)



(a)

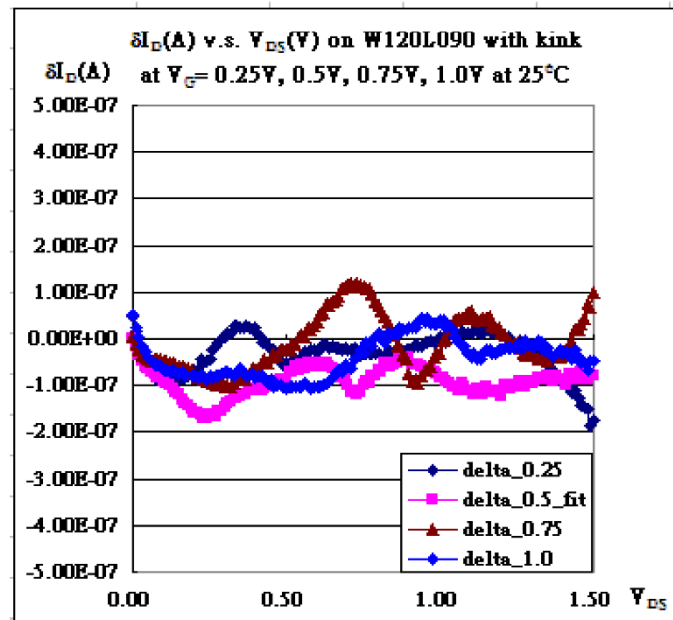
(b) $\delta_{0.25}=5.28 \times 10^{-8}$, $\delta_{0.5}=9.78 \times 10^{-8}$, $\delta_{0.75}=6.06 \times 10^{-8}$, $\delta_{1.0}=5.88 \times 10^{-8}$

Figure 7. 0.090 micron process (a) I_{DS} - V_{DS} characteristic curves and the corresponding fitting by turning on kink-effect factor. (b) the corresponding fitting with improved minimum delta (δ)

Author Contributions: Conceptualization, H.C. Yang., and S.C. Chi.; methodology, H.C. Yang., and S.C. Chi.; software, H.C. Yang., and S.C. Chi.; validation, H.C. Yang., and S.C. Chi.; formal analysis, H.C. Yang., and S.C. Chi.; investigation, H.C. Yang., and S.C. Chi.; resources, H.C. Yang., and S.C. Chi.; data duration, H.C. Yang., and S.C. Chi.;

Funding: Not available

Institutional Review Board Statement: Not available

Informed Consent Statement: Not available

Data Availability Statement: No

Conflicts of Interest: No

References

1. Diab, A.; Torres Sevilla, G.-A.; Christoloveanu, S.; and Hussain, M.-M. Room to high temperature measurements of flexible SOI FinFETs with sub-20-nm fins. *IEEE Trans. Electron. Devices* **2014**, *61*, 3978.
2. Wang, F.; Xie, Y.; Bernstein, K.; Luo, Y. Dependability analysis of nano-scale FinFET circuits. In Proceedings of the IEEE Computer Society Annual Symposium on Emerging VLSI Technologies and Architectures (ISVLSI'06), Karlsruhe, Germany, 2–3 March **2006**; pp 6, 399.
3. Huang, X.; Lee, W.-C.; Kuo, C.; Hisamoto, D.; Chang, L.; Kedzierski, J.; Anderson, E.; Takeuchi, H.; Choi, Y.-K.; Asano, K.; et al. Sub-50 nm P-channel FinFET. *IEEE Trans. Electron. Devices* **2001**, *48*, 880.
4. Rudenko, T., Kilchytska, V., Arshad, M.K.M., Raskin, J.-P., Nazarov, A. and Flandre, D. On the MOSFET Threshold Voltage Extraction by Transconductance and Transconductance-to-Current Ratio Change Methods: Part II-Effect of Drain Voltage. *IEEE Trans. Electron. Devices* **2011**, *58*, 4180–4188.
5. Takahashi, T.; Beppu, N.; Chen, K.; Oda, S.; Uchida, K. Self-heating effects and analog performance optimization of Fin-type field-effect transistors. *Jpn. J. Appl. Phys.* **2013**, *52*, 04CC03.
6. Saitoh, M.; Yasutake, N.; Nakabayashi, Y.; Uchida, K.; Numata, T. Understanding of strain effects on high-field carrier velocity in (100) and (110) CMOSFETs under quasi-ballistic transport. 2009 IEEE International Electron Devices Meeting (IEDM), Baltimore, MD, USA, 07–09 December **2009**; pp. 1–4.
7. Chen, C.W.; Wang, S.J.; Hsieh, W.C.; Chen, J.M.; Jong, T.; Lan, W.H.; Wang, M.C. Q-factor Performance of 28 nm-node High-k Gate Dielectric under DPN Treatment at Different Annealing Temperatures. *Electronics* **2020**, *9*, 2086.
8. Lu, P.; Yang, C.; Li, Y.; Li, B.; Han, Z. Three-Dimensional TID Hardening Design for 14 nm Node SOI FinFETs. *Eng* **2021**, *2*, 620–631.
9. Song, Y.S.; Tayal, S.; Rahi, S.B.; Kim, J.H.; Upadhyay, A.K.; Park, B.-G. Thermal-Aware IC Chip Design by Combining High Thermal Conductivity Materials and GAA MOSFET. In Proceedings of the 2022 5th International Conference on Circuits, Systems and Simulation (ICCS), Nanjing, China, 13–15 May **2022**; pp. 135–140.
10. Crupi, G.; Schreurs, D.M.M.-P.; Caddemi, A.; Angelov, I.; Homayouni, M.; Raffo, A.; Vannini, G.; Parvais, B. Purely analytical extraction of an improved nonlinear FinFET model including non-quasi-static effects. *Microelectron. Eng.* **2009**, *86*, 2283–2289.
11. Li, Y.; Zhao, F.; Cheng, X.; Liu, H.; Zan, Y.; Li, J.; Zhang, Q.; Wu, Z.; Luo, J.; Wang, W. Four-Period Vertically Stacked SiGe/Si Channel FinFET Fabrication and Its Electrical Characteristics. *Nanomaterials* **2021**, *11*, 1689.
12. Zhao, E.; Zhang, J.; Salman, A.; Subba, N.; Chan, J.; Marathe, A.; Beebe, S.; Taylor, K. Reliability challenges of high performance PD SOI CMOS with ultra-thin gate dielectrics. *Solid State Electron.* **2004**, *48*, 1703–1708.
13. Zhao, Z.Q.; Li, Y.; Zan, Y.; Li, Y.L.; Li, J.J.; Cheng, X.H.; Wang, G.L.; Liu, H.Y.; Wang, H.X.; Zhang, Q.Z.; et al. Fabrication technique of the Si_{0.5}Ge_{0.5} Fin for the high mobility channel FinFET device. *Semicond. Sci. Technol.* **2020**, *35*, 045015.
14. Lee, J.; Park, T.; Ahn, H.; Kwak, J.; Moon, T.; Shin, C. Prediction Model for Random Variation in FinFET Induced by Line-Edge-Roughness (LER). *Electronics* **2021**, *10*, 455.
15. Yang, H.-C.; Chi, S.-C. Process Corresponding Implications Associated with a Conclusive Model-Fit Current-Voltage Characteristic Curves. *Appl. Sci.* **2022**, *12*, 462
16. Yang, H.-C.; Chi, S.-C.; Liao W.S. Comparison of Fitting Current–Voltage Characteristics Curves of FinFET Transistors with Various Fixed Parameter. *Appl. Sci.* **2022**, *12*, 10519
17. Lewis H. Ryder, Quantum Field Theory, Chapter 10.1 The sine-Gordon kink, p402, Published by the Press Syndicate of the University of Cambridge. ISBN 0 521 23764 5 hard covers
18. D. Lacroix, I. Traore, S. Fumwron, and G. Jeandel. Phonon transport in silicon, influence of the dispersion properties choice on the description of the anharmonics resistive mechanisms. *Eur. Phys. J. B* **67** 15–25,(2009)

Disclaimer/Publisher's Note: The statements, opinions and data contained in all publications are solely those of the individual author(s) and contributor(s) and not of MDPI and/or the editor(s). MDPI and/or the editor(s) disclaim responsibility for any injury to people or property resulting from any ideas, methods, instructions or products referred to in the content.